Supporting Information for

# Suppressing the Voltage Decay of Low-Cost P2-Type Iron Based Cathode Materials for Sodium-ion Batteries

*Shuyin Xu,[‡ab] Jinpeng Wu,[‡d] Enyuan Hu,[c] QinghaoLi,[a] Jienan Zhang,[a] Yi Wang,[a] Eli Stavitski,[c] Liwei Jiang,[a] Xiaohui Rong,[a] Xiqian Yu,[*a] Wanli Yang,[d] Xiao-Qing Yang,[*c] Liquan Chen[a] and Yong-Sheng Hu*[a]*

a. *Key Laboratory for Renewable Energy, Beijing Key Laboratory for New Energy Materials and Devices, Beijing National Laboratory for Condensed Matter Physics, Institute of Physics, Chinese Academy of Sciences, School of Physical Sciences, University of Chinese Academy of Sciences, Beijing 100190, China. *E-mail: xyu@iphy.ac.cn; yshu@iphy.ac.cn*
b. *Key Laboratory of Semiconductor Photovoltaic Technology of Inner Mongolia Autonomous Region, School of Physical Science and Technology, Inner Mongolia University, Hohhot 010021, China.*
c. *A Brookhaven National Laboratory, Upton, New York 11973, USA. *E-mail: xyang@bnl.gov*
d. *Advanced Light Source, Lawrence Berkeley National Laboratory, Berkeley, CA 94720, USA*

‡ S.Y. Xu and J.P. Wu contributed equally to this work.

**Supporting Figures**

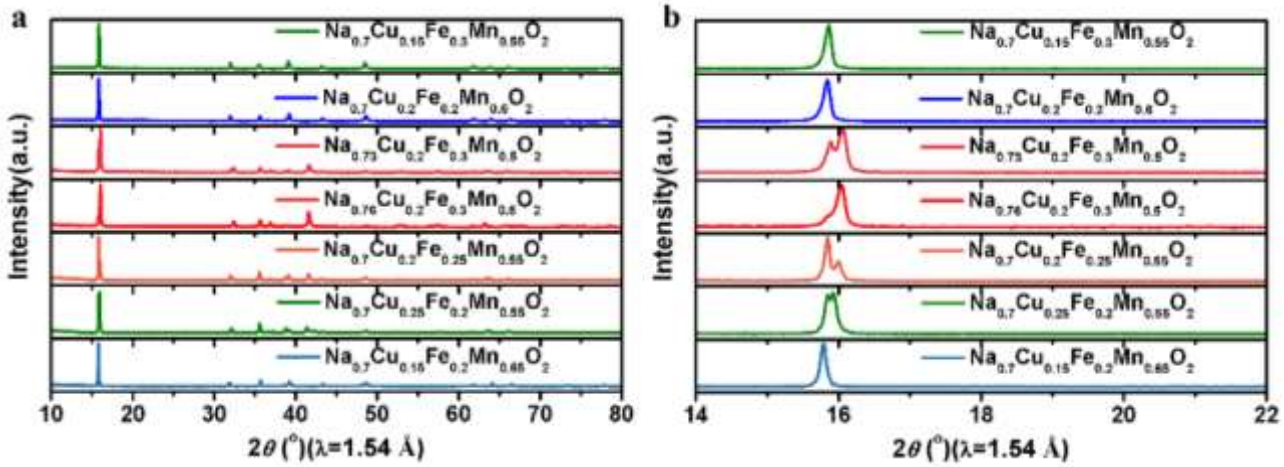


**Figure S1.** X-ray diffraction patterns. The XRD patterns of the as-prepared materials with different Na, Cu, Fe, Mn composition at a scanning range of a)10-80$^{o}$ and b)14-22$^{o}$.

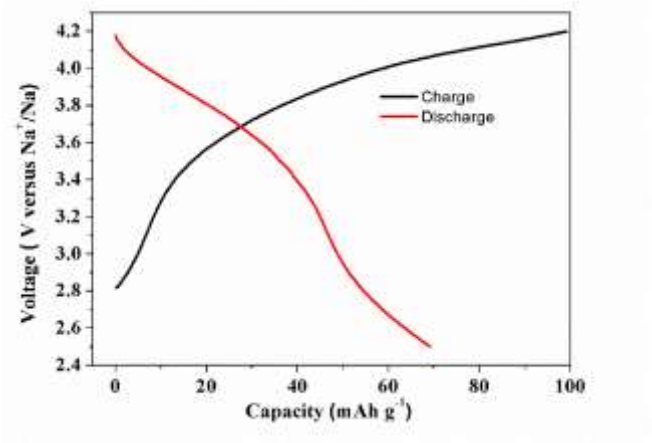


**Figure S2.** The first charge and discharge curves of the P2-type $Na_{0.7}Cu_{0.15}Fe_{0.2}Mn_{0.65}O_2$

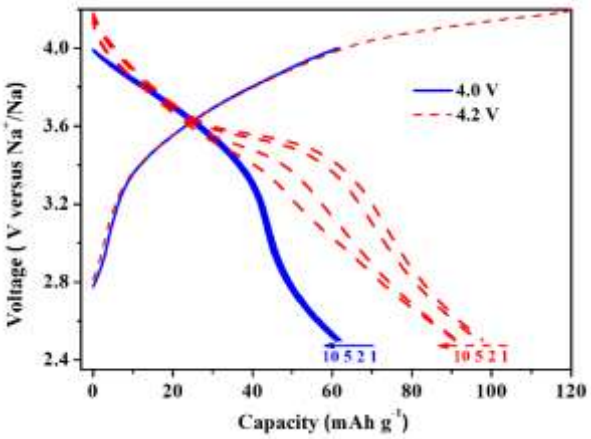


**Figure S3.** The charge and discharge curves of the $Na_{0.7}Cu_{0.15}Fe_{0.3}Mn_{0.55}O_2$ cycled between 2.5-4.0 V and 2.5-4.2 V.

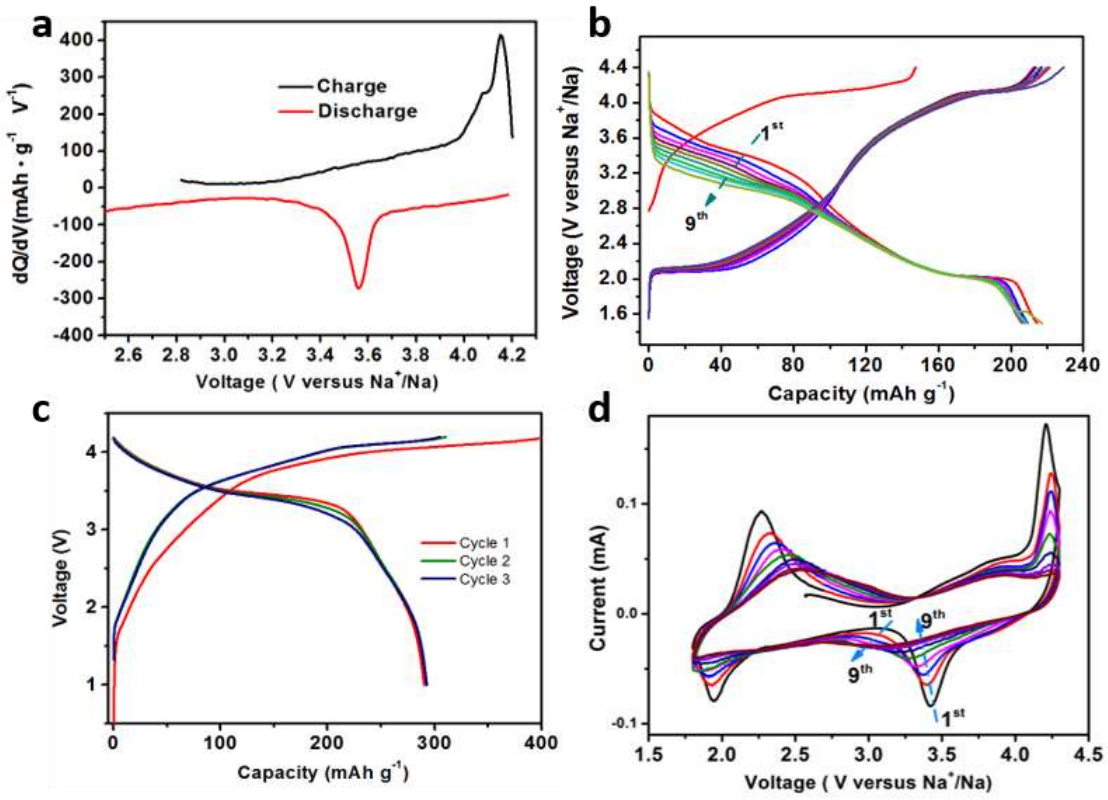


**Figure S4.** Typical electrochemical performance of $Na_{0.7}[Cu_{0.15}Fe_{0.3}Mn_{0.55}]O_2$. **a)** the differential capacity (dQ/dV) plots corresponding to the first charge and discharge profiles. **b)** Charge and discharge profiles of $Na_{0.7}[Cu_{0.15}Fe_{0.3}Mn_{0.55}]O_2$ galvanostatically measured at the C/10 rate in the voltage ranges of 1.5- 4.4 V. **c)** Sodium storage performance of the $Na_{0.7}[Cu_{0.15}Fe_{0.3}Mn_{0.55}]O_2$ //Hard carbon full cells. **d)** Cyclic voltammograms of $Na_{0.7}[Cu_{0.15}Fe_{0.3}Mn_{0.55}]O_2$ in the potential range from 1.6 to 4.3 V ($Na^+$/Na).

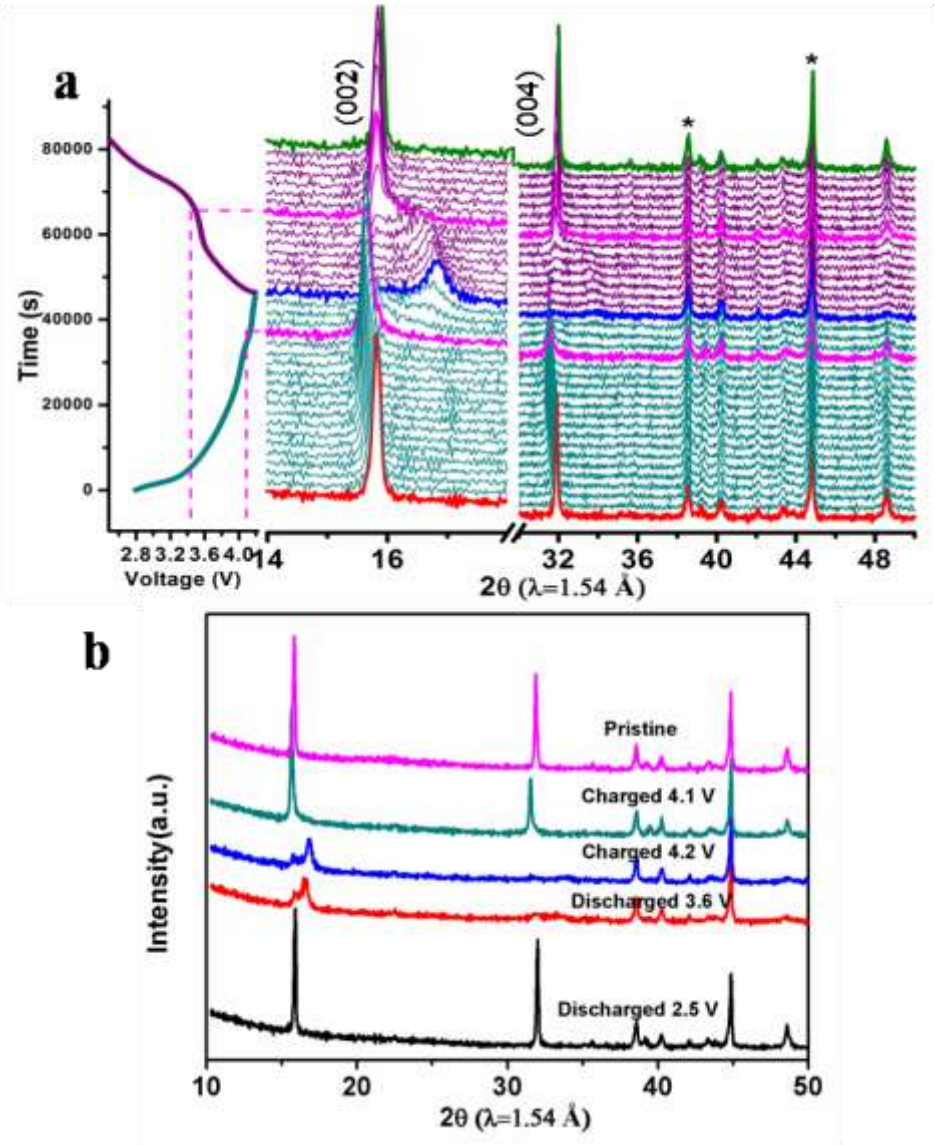


**Figure S5.** Structure evolution during Na extraction and insertion. **a)** In situ XRD patterns collected during the first charge/discharge of $Na_{0.7}[Cu_{0.15}Fe_{0.3}Mn_{0.55}]O_2$ electrode cycled between 2.5 and 4.2 V under a current rate of C/15. Black asterisks represent peaks from Al window. **b)** Five XRD patterns selected from the in situ XRD datas.

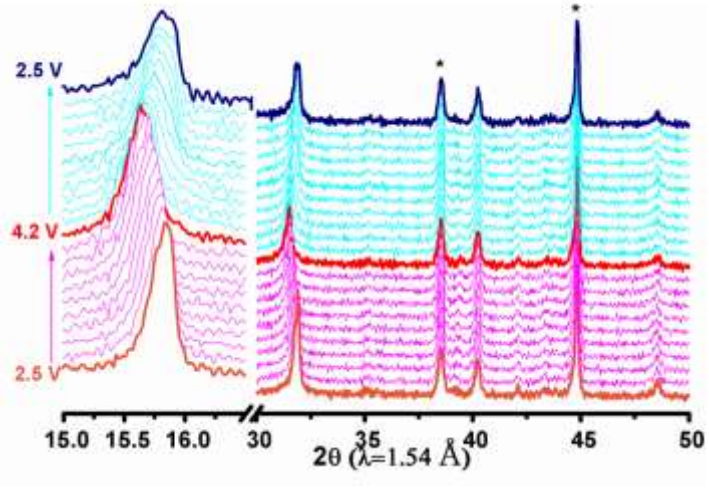


**Figure S6.** Structure evolution during Na extraction and insertion. In situ XRD patterns collected during the 15$^{th}$ charge/discharge of $Na_{0.7}[Cu_{0.15}Fe_{0.3}Mn_{0.55}]O_2$ electrode cycled between 2.5 and 4.2 V under a current rate of C/15. Black asterisks represent peaks from Al window.

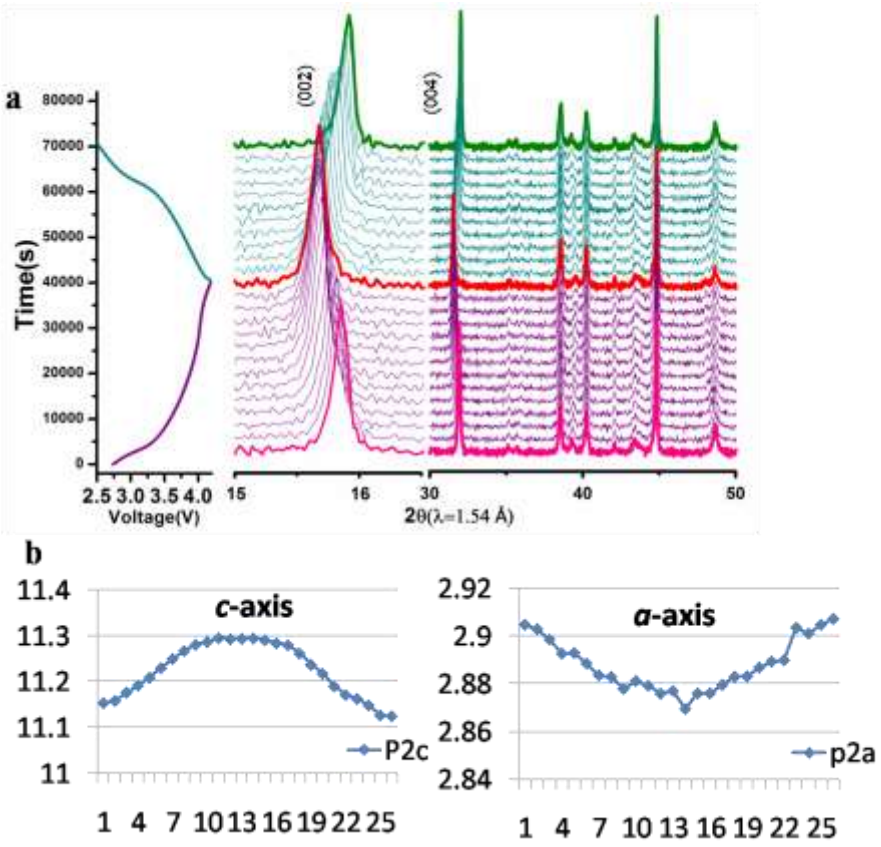


**Figure S7.** Structure evolution during Na extraction and insertion. **a)** In situ XRD patterns collected during the first charge/discharge process of $Na_{0.7}[Cu_{0.2}Fe_{0.2}Mn_{0.6}]O_2$ electrode cycled between 2.5 and 4.2 V under a current rate of C/15. Black asterisks represent peaks from Al window. **b)** Evolution of the average interlayer distance (*c*-axis) and in-plane lattice parameter (*a*-axis).

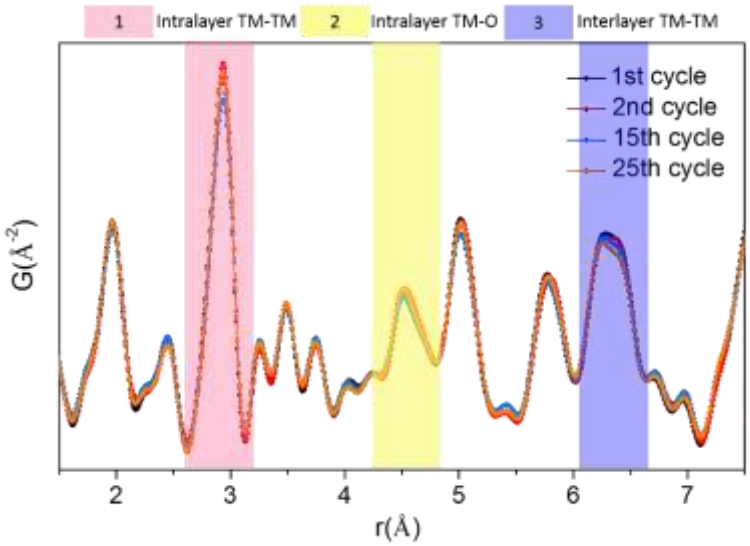


**Figure S8.** Comparison of the experimental PDF data of $Na_{0.7}[Cu_{0.2}Fe_{0.2}Mn_{0.6}]O_2$ with different charge-discharge cycles. First neighbor intralayer TM–TM and second neighbor intralayer TM–O distances in-plane are highlighted in lavender and yellow respectively, and interlayer TM–TM distances are highlighted in light purple.

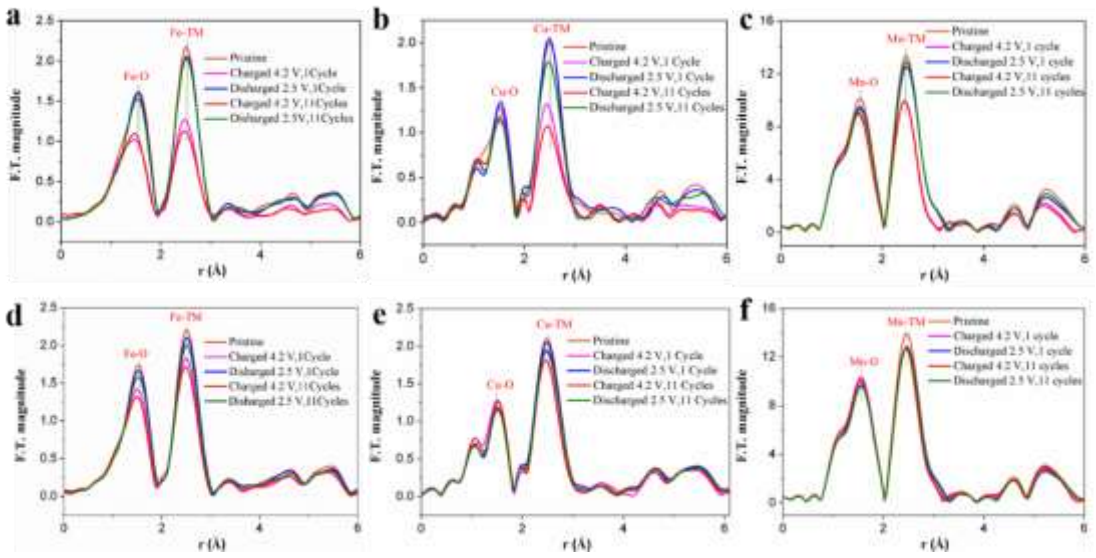


**Figure S9.** XAS results. The EXAFS spectra of the of **a-c)** $Na_{0.7}[Cu_{0.15}Fe_{0.3}Mn_{0.55}]O_2$ and **d-f)** $Na_{0.7}[Cu_{0.2}Fe_{0.2}Mn_{0.6}]O_2$ electrodes at different SOCs during the 1$^{st}$ and the 11$^{th}$ cycles: **a)**, **d)** Fe ion **b)**, **c)** Cu ion, **e)**, **f)** Mn ion.

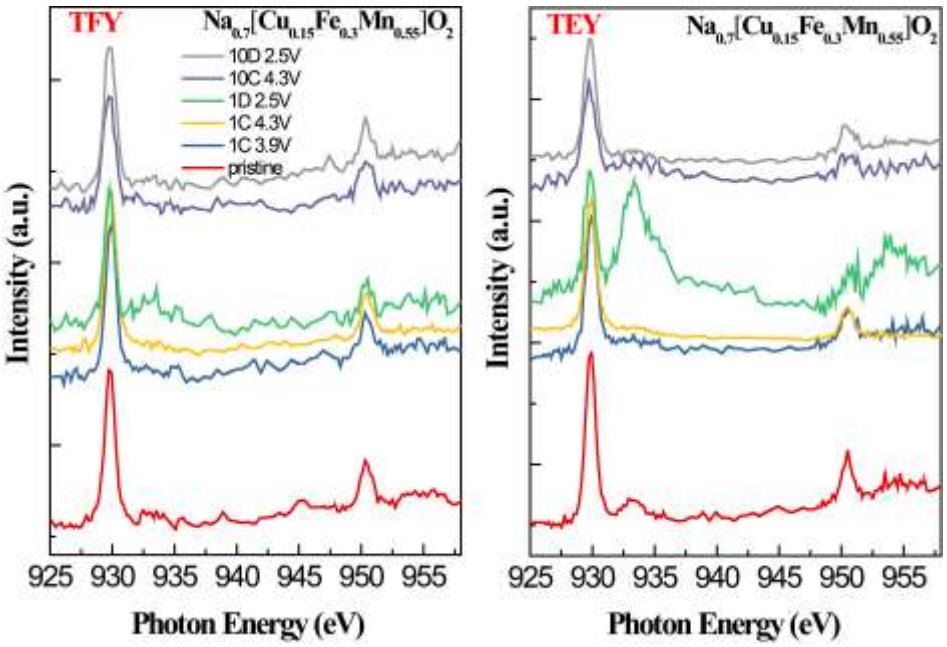


**Figure S10.** Cu-L edge sXAS on $Na_{0.7}[Cu_{0.15}Fe_{0.30}Mn_{0.55}]O_2$ cathode at different cycle states. sXAS are collected in both bulk sensitive TFY mode and surface sensitive TEY mode.

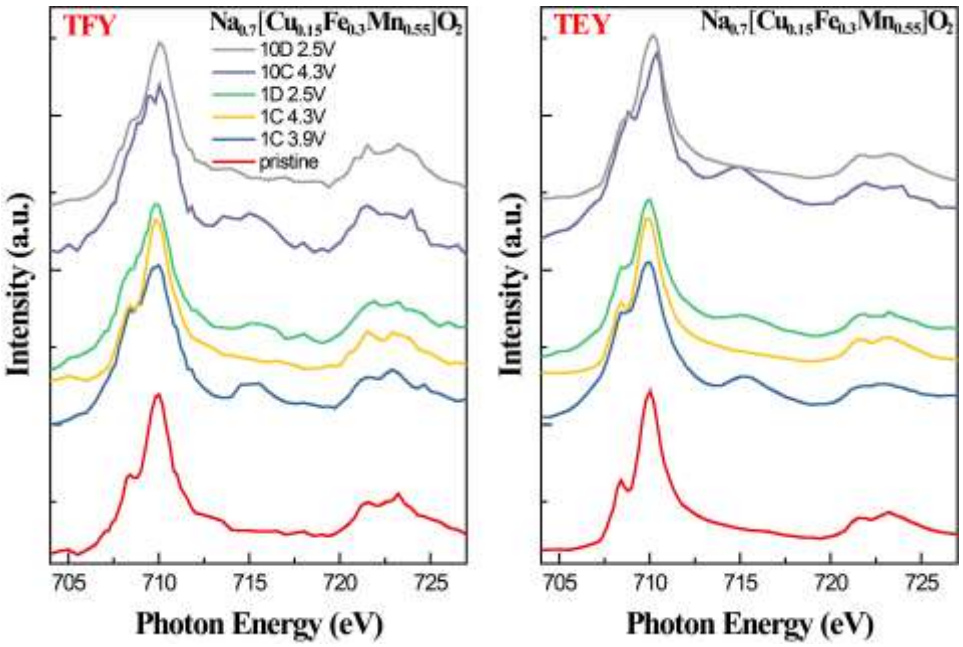


**Figure S11.** Fe-L edge sXAS on $Na_{0.7}[Cu_{0.15}Fe_{0.30}Mn_{0.55}]O_2$ cathode at different cycle states. sXAS are collected in both bulk sensitive TFY mode and surface sensitive TEY mode.

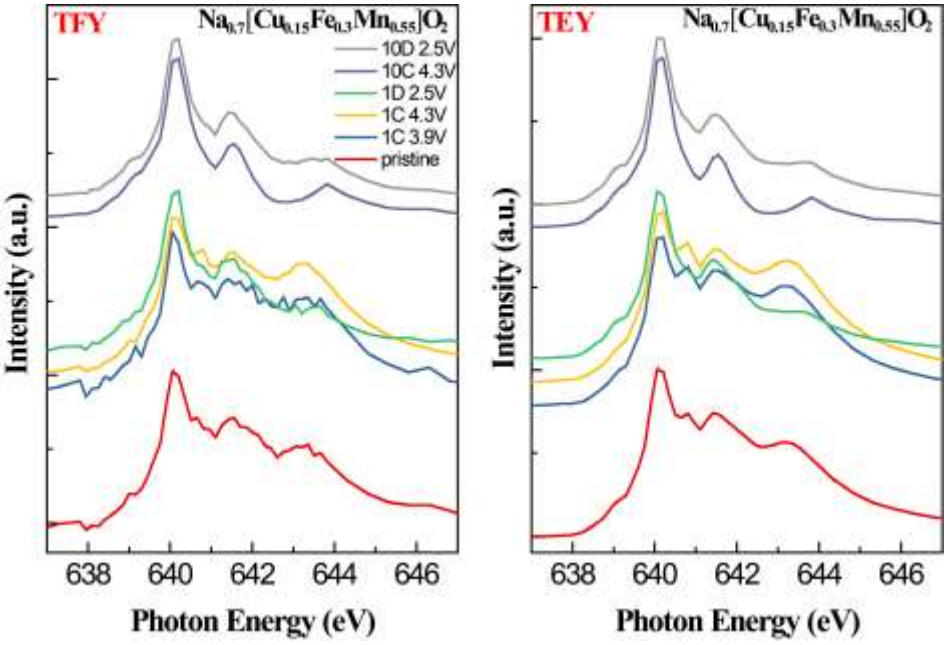


**Figure S12.** Mn-L edge sXAS on $Na_{0.7}[Cu_{0.15}Fe_{0.30}Mn_{0.55}]O_2$ cathode at different cycle states. sXAS are collected in both bulk sensitive TFY mode and surface sensitive TEY mode.

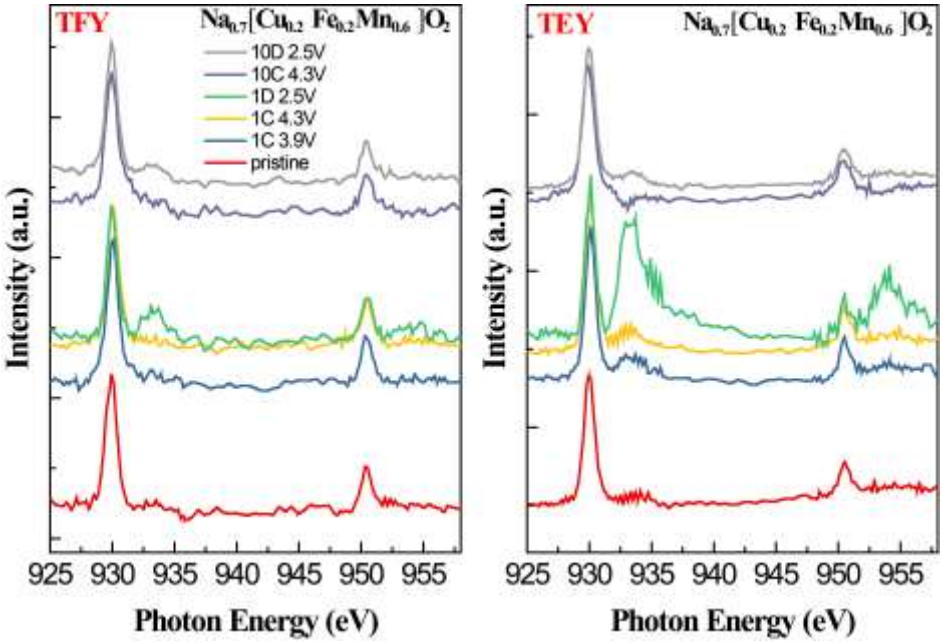


**Figure S13.** Cu-L edge sXAS on $Na_{0.7}[Cu_{0.20}Fe_{0.20}Mn_{0.60}]O_2$ cathode at different cycle states. sXAS are collected in both bulk sensitive TFY mode and surface sensitive TEY mode.

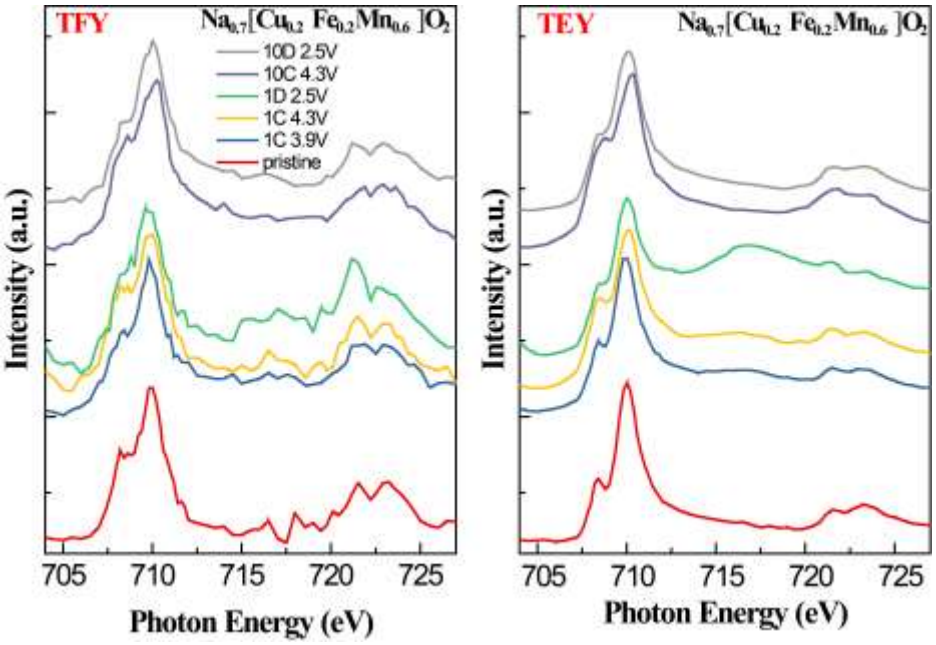


**Figure S14.** Fe-L edge sXAS on $Na_{0.7}[Cu_{0.20}Fe_{0.20}Mn_{0.60}]O_2$ cathode at different cycle states. sXAS are collected in both bulk sensitive TFY mode and surface sensitive TEY mode.

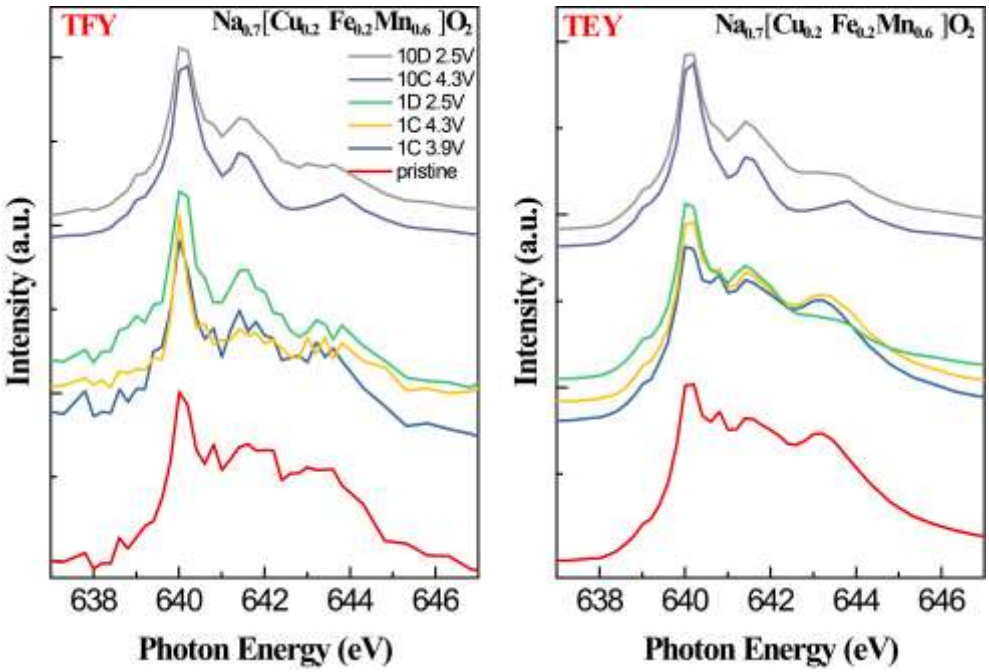


**Figure S15.** Mn-L edge sXAS on $Na_{0.7}[Cu_{0.20}Fe_{0.20}Mn_{0.60}]O_2$ cathode at different cycle states. sXAS are collected in both bulk sensitive TFY mode and surface sensitive TEY mode.

**Supporting Tables**

**Table S1.** Summary of the structure parameters of $Na_{0.7}[Cu_xFe_yMn_{1-x-y}]O_2$ determined from the Rietveld refinement.

| | a(b) | c | volume | Rwp | Rp | $\chi^2$ |
|---|---|---|---|---|---|---|
| $Na_{0.7}[Cu_{0.15}Fe_{0.3}Mn_{0.55}]O_2$ | 2.91968(9) | 11.18707(26) | 82.588(4) | 10.79 | 7.94 | 1.748 |
| $Na_{0.7}[Cu_{0.20}Fe_{0.2}Mn_{0.60}]O_2$ | 2.91040(12) | 11.18935(33) | 82.081(5) | 10.52 | 7.17 | 2.017 |